Packing size effect on the liquid circulation property in an external-loop packed bubble column

Yanling Tang, Gang Luo, Zhenmin Cheng*

State Key Laboratory of Chemical Engineering, School of Chemical Engineering, East China University of Science and Technology, Shanghai 200237, China

Abstract

Packing size effects on the fluid dynamics in an external-loop packed bubble column with Raschig rings of three different effective diameters (5, 14 and 41 mm) in the riser were investigated. The overall gas holdup, liquid circulating velocity and gas-liquid mass transfer coefficient were respectively measured by volume expansion method, tracer-response method and dynamic oxygen-absorption technique. CFD simulation with the Euler-Euler two-fluid method was used to predict the liquid circulating velocity by treating the packing as a porous medium. Compared to the empty column, the gas holdup was found to increase with the presence of packing, however, the liquid circulating velocity and gas-liquid mass transfer coefficient may increase or decrease. Specifically, the gas holdup increases with the decrease of packing size, while the liquid circulating velocity is on the contrary, which induces the maximal gas-liquid mass transfer rate at packing diameter of 14 mm.

Keywords: external-loop packed bubble column; gas holdup; liquid circulating velocity; gas-liquid mass transfer.

---

*Corresponding author. Email: zmcheng@ecust.edu.cn

1. Introduction

Packed bubble columns with concurrent gas-liquid upward flow are widely used in the chemical industry. The packing size may greatly affect the hydrodynamics in the column by inducing bubble coalescence or breakup (Jo and Revankar, 2009; Jo and Revankar, 2010). Generally speaking, the gas holdup and mean bubble diameter increase with the packing size (Sivakumar et al., 1999; Bordas et al., 2006; Chen et al., 2017). Although reducing the packing size can increase the catalyst loading capacity and internal effectiveness factor (Ling et al., 2017), for fine particles ($d_p \leq 2\mathrm{mm}$), the gas maldistribution and slug formation would occur (Lamine et al., 1995; Moreira and Freire, 2003; Collins et al., 2017). In the work of Deshpande et al (2018), the smallest acceptable packing size is suggested in the consideration of gas-liquid mass transfer, since below which gas bubble coalescence is likely to dominate.

The packing size would be more important for an external-loop packed bubble column with the packing in the riser, which can be used in a three-phase system carrying out gas-phase strong exothermic reaction, while the liquid is recycled to overcome the heat removal problem. Compared to the conventional packed bubble column in which the liquid phase must be introduced into the reactor by a pump, the automatically external recycling of the liquid would be realized from the density difference between the riser and downcomer in an external-loop packed bubble column.

Regrettably, most of the current studies on the three-phase external-loop reactors are primarily on fluidized beds (Guo et al., 1997; Papalas et al., 2020; Pronczuk and Bizon, 2019) and slurry beds (Liu et al., 2008; Milivojevic et al., 2012; Bian et al., 2016;

Geng et al., 2020). There are only few reports in the open literature concerning the external-loop packed beds, and almost all of them are about bioreactors, in which the presence of packing is used to improve the residence time or increase cell attachment area. Thus, the packing used in the riser has an extremely high porosity to reduce liquid circulation resistance, for example, fiberglass (Hamood-ur-Rehman et al., 2012a, b), woven nylon (Meng et al., 2002), stainless steel mesh (Nikakhtari and Hill, 2005a, b, c), are mostly used, which are quite different from the catalyst used in chemical industry.

Based on 2 mm Raschig ring and glass sphere as the packing, Chisti and Moo-Young (1993) developed an energy balance approach to predict the liquid circulating velocity. In their subsequent studies, they used an airlift packed-bed in the large scale culture of anchorage dependent animal cells, and they found that such a reactor can support 2.76-fold cell concentration compared to the stirred tank having the same volume (Chisti and Moo-Young, 1994). However, the packing was placed in the downcomer, and the packing loading method has been widely followed in the later studies (Silapakul et al., 2005; Jalilnejad and Vahabzadeh, 2014).

In this study, liquid external circulation fluid dynamics property will be systematically investigated in an air-lift external-loop packed bubble column loaded with Raschig rings of three different effective diameters (5, 14 and 41 mm) packed in the riser. Liquid flow trajectory is traced by red ink. The overall gas holdup, liquid circulating velocity and gas-liquid mass transfer coefficient are respectively measured by volume expansion method, tracer-response method and dynamic oxygen-absorption technique. Moreover, a simulation with the Euler-Euler two-fluid method is used to predict the liquid circulating velocity by treating the packing as porous medium (Atta et al., 2007; Lappalainen et al., 2009; Lappalainen et al., 2011; Solomenko et al., 2015). The effects of superficial gas velocity, downcomer diameter and packing size on the fluid dynamics are under consideration.

2 Materials and methods

2.1 Experiment setup

The experimental setup shown in Fig. 1 consists of three parts: a riser, a downcomer, and a gas-liquid separator. The riser and downcomer were connected by an inclined tube at the bottom. The diameter of the riser (D_r) was fixed at 0.26 m, while the diameter of downcomer (D_c) varied in 0.05 m, 0.08 m and 0.10 m. The heights of the riser and downcomer were 1.9 m and 1.5 m, respectively. A gas distributor was located at a distance of 0.4 m from the bottom of the riser to ensure uniform inlet distribution of gas and provide supporting of the packing. Raschig rings of same size (see in table 1) with a packing height of 1.2 m were loaded randomly in the riser. The superficial gas velocity (U_g) variation range was from 0.01 to 0.052 m/s.

Table 1 Raschig rings geometrical parameters

Packing material	External diameter×Height×Wall thickness mm×mm×mm	Effective particle diameter d_p / mm	Bed porosity ε
ceramics	6×4×1	5	0.6
	15×15×2.5	14	0.7
	50×50×5	41	0.8

The overall gas holdup (β_g) was measured by the classical volume expansion method (Moraveji et al., 2013), and the tracer-response method was used to obtain liquid circulating velocity in the downcomer ($u_{l,c}$) and liquid circulating volume flow rate (Q_l). Two high frequency conductivity probes were placed 1.46 m apart in the downcomer, the tracer (10 ml, saturated KCl) was instantaneously injected at the top of downcomer. $u_{l,c}$ was calculated from the distance between the two conductivity probes divided by the travel time of tracer through them, and Q_l was the product of downcomer sectional area and the velocity $u_{l,c}$.

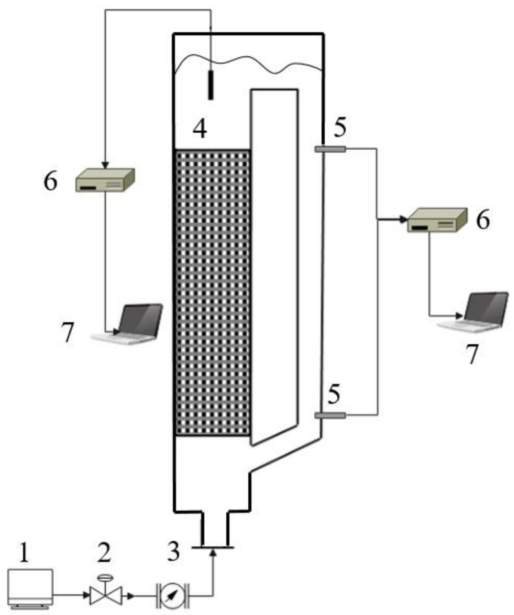

Fig. 1 Schematic diagram of the experimental setup

1. Air compressor 2. Valve 3. Flowmeter 4. Oxygen probe
5. Conductivity probe 6. A/D adaptor 7. Data acquisition

The volumetric gas-liquid mass transfer coefficient ($k_l a$) was estimated by a dynamic oxygen-absorption technique. The oxygen in the water was first purged with Na_2SO_3, then, the air was pumped into the external-loop reactor, with a dissolved oxygen (DO) probe monitoring the dissolved oxygen concentration variation with time.

From the DO profile, $k_l a$ with negligible electrode response time (Guo et al., 1997; Fakhari et al., 2014; Moraveji and Gharib, 2014) is obtained:

$$\ln\left(\frac{C^{*}-C_{1}}{C^{*}-C_{0}}\right)=-k_{1}at \quad (1)$$

Where, C_l is the instantaneously dissolved oxygen concentration at time t, respectively, C^* is the saturated oxygen concentration, C_0 is the initial oxygen concentration. By plotting $\ln\left(\frac{C^{*}-C_{1}}{C^{*}-C_{0}}\right)$ versus t, $k_l a$ is be solved by parameter fitting.

2.2 CFD simulation on the liquid circulation

Euler-Euler approach is used to simulate the fluid dynamics in the external-loop packed bubble column with module of porous media by ANSYS Fluent software package. Initially, the reactor is set to be filled with static liquid of 2 m in height, then, the gas enters the reactor through the inlet at the bottom of the riser, leading to inception of an automatically external circulation of the liquid.

The volume-averaged equations for gas and liquid can be written in the following formula.

The mass balance equation,

$$\frac{\partial}{\partial t}\left(\beta_{g}\rho_{g}\right)+\nabla\cdot\left(\beta_{g}\rho_{g}\overrightarrow{u_{g}}\right)=0 \quad (2)$$

$$\frac{\partial}{\partial t}\left(\beta_{l}\rho_{l}\right)+\nabla\cdot\left(\beta_{l}\rho_{l}\overrightarrow{u_{l}}\right)=0 \quad (3)$$

Momentum balance equation,

$$\frac{\partial}{\partial t}\left(\beta_{g}\rho_{g}\overrightarrow{u_{g}}\right)+\nabla\cdot\left(\beta_{g}\rho_{g}\overrightarrow{u_{g}}\overrightarrow{u_{g}}\right)=-\beta_{g}\nabla\vec{p}+\nabla\cdot\left(\beta_{g}\overline{\overline{\tau_{g}}}\right)+\beta_{g}\rho_{g}\vec{g}+\overrightarrow{F_{g,l}}+\overrightarrow{F_{g,s}} \quad (4)$$

$$\frac{\partial}{\partial t}\left(\beta_{l}\rho_{l}\overrightarrow{u_{l}}\right)+\nabla\cdot\left(\beta_{l}\rho_{l}\overrightarrow{u_{l}}\overrightarrow{u_{l}}\right)=-\beta_{l}\nabla\vec{p}+\nabla\cdot\left(\beta_{l}\overline{\overline{\tau_{l}}}\right)+\beta_{l}\rho_{l}\vec{g}+\overrightarrow{F_{l,g}}+\overrightarrow{F_{l,s}} \quad (5)$$

Where, β_k is the phase volume fraction, ρ_k is the density, the $\overrightarrow{u_k}$ is the velocity, $\vec{p}$ is the pressure, $\overline{\overline{\tau_k}}$ is the average stress tensor, $\vec{g}$ is the gravitational acceleration, $\overrightarrow{F_{g,l}}$ and $\overrightarrow{F_{l,g}}$ are the drag force in the gas-liquid flows, $\overrightarrow{F_{g,s}}$ and $\overrightarrow{F_{l,s}}$ refer, respectively, to gas-solid and liquid-solid interaction forces due to porous resistances.

In the porous media domain with packing, the packing resistances on gas and liquid phases write as follows by viewing packing bed as isotropic porous media (Boyer et al., 2007):

$$\overrightarrow{F_{k,s}} = K_{ks}\overrightarrow{u_k} \tag{6}$$

In above equation, fluid-solid momentum exchange coefficients K_{ks} are expressed by follows:

$$K_{gs} = E_1\mu_g \frac{\left(1-\beta_g\right)^2}{\beta_g d_p^2}\left(\frac{1-\varepsilon}{1-\beta_g}\right)^{2/3} + E_2\rho_g \frac{1-\beta_g}{d_p}\left(\frac{1-\varepsilon}{1-\beta_g}\right)^{1/3}\left\|\overrightarrow{u_g}\right\| \tag{7}$$

$$K_{ls} = E_1\mu_l \frac{\left(1-\varepsilon\right)^2}{\beta_l d_p^2} + E_2\rho_l \frac{1-\varepsilon}{d_p}\left\|\overrightarrow{u_l}\right\| \tag{8}$$

Gas-liquid interaction force contains viscous and inertial contributions as well and writes as follows

$$\overrightarrow{F_{gl}} = K_{gl}\left(\overrightarrow{u_g} - \overrightarrow{u_l}\right) \tag{9}$$

where K_{gl} is a gas-liquid interaction coefficient that writes as follows:

$$K_{gl} = E_1\mu_g \frac{\left(1-\beta_g\right)^2}{\beta_g d_p^2}\left(\frac{1-\varepsilon}{1-\beta_g}\right)^{2/3} + E_2\rho_g \frac{1-\beta_g}{d_p}\left(\frac{1-\varepsilon}{1-\beta_g}\right)^{1/3}\left\|\overrightarrow{u_g} - \overrightarrow{u_l}\right\| \tag{10}$$

In Eqs. (7), (8) and (10), E_1 and E_2 are taken equal to 150 and 1.75, which are fitted by a large number of experiments (Boyer et al., 2007), ε is the bed porosity, and d_p is effective particle diameter.

In the free fluid domain without packing, $\overrightarrow{F_{k,s}}$ is set as zero, and $\overrightarrow{F_{gl}}$ can be written as

$$\overrightarrow{F_{gl}} = C_D \pi d_{\mathrm{b}}^{\ 2} \frac{\rho_l}{8} \left\| \overrightarrow{u_g} - \overrightarrow{u_l} \right\| \left(\overrightarrow{u_g} - \overrightarrow{u_l} \right) \tag{11}$$

Where, d_{b} is the bubble diameter, C_D is the drag coefficient, which follow the Ishii-Zuber model (Ishii and Zuber, 1979):

$$C_D = \frac{2}{3} Eo^{1/2} \tag{12}$$

Eo is Eötvös number, defined by

$$Eo = \frac{g\left(\rho_l - \rho_g\right) d_{\mathrm{b}}}{\sigma} \tag{13}$$

Where, σ is gas-liquid surface tension.

3 Results and discussions

3.1. Visual observation

In order to verify whether the designed structure can achieve liquid external circulation, 10 mL red ink was used as a tracer to obtain the liquid flow trajectory when the superficial gas velocity is 0.052 m/s and downcomer diameter is 0.08 m, which is shown in Fig. 2. It can be seen that, compared with empty column, the liquid circulating velocity is slower and the liquid circulation time is longer in the packed bubble column, and the effect is more significant when the packing size is reduced. However, even when the effective packing size is 5 mm, the liquid external circulation can be realized with highest flow resistance.

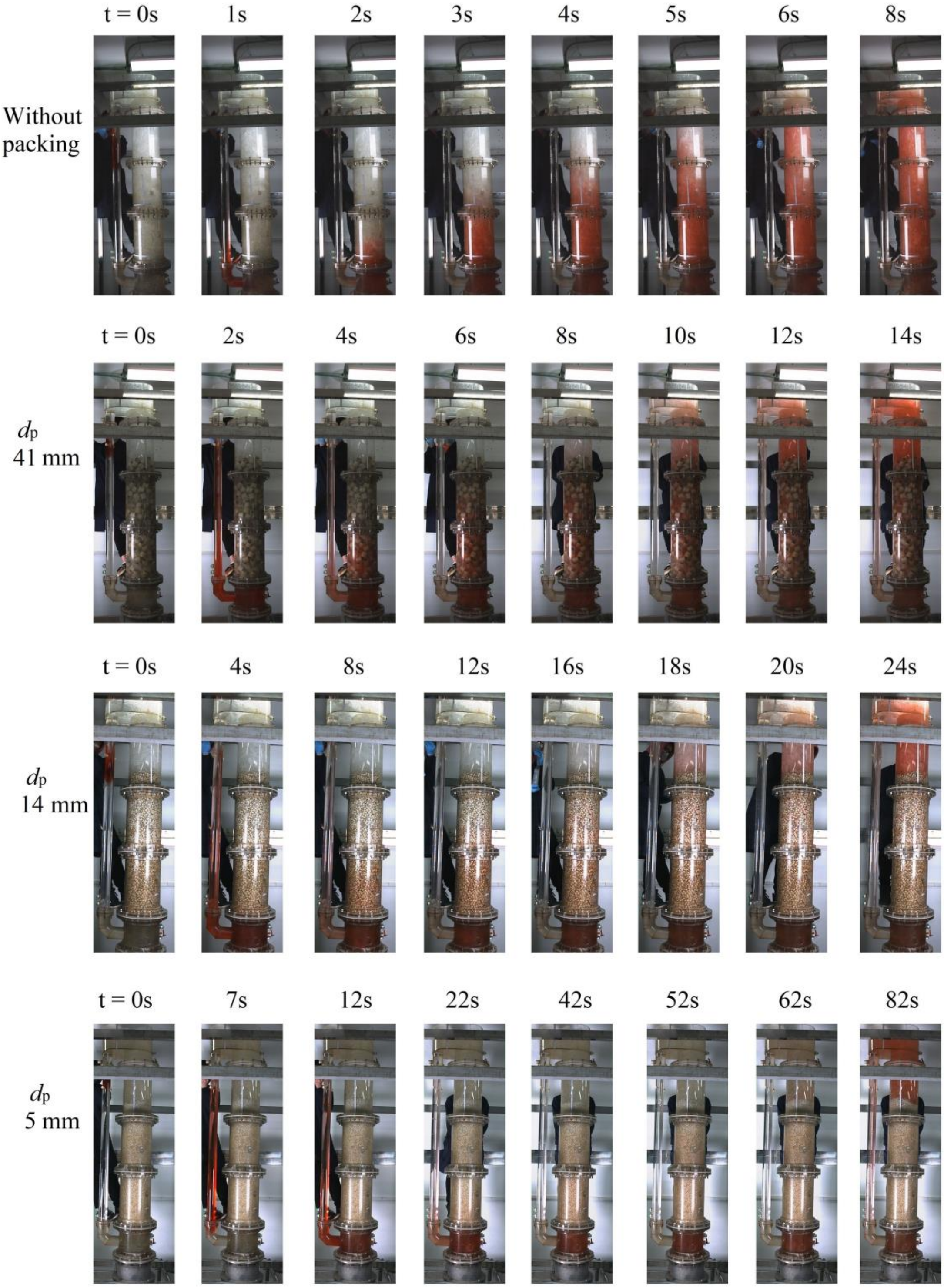

Fig. 2 The liquid flow trajectory in the reactor with the red ink as a tracer

3.2 Gas holdup

Gas holdup is a key important parameter in the external-loop packed bubble column, as the difference of gas holdup between the riser and downcomer is the driving force of liquid circulation (Geng et al., 2020). The gas holdup determines liquid circulating velocity and mixing time (Dhaouadi et al., 2006). What is more, the gas holdup is also directly related to the gas-liquid mass transfer (Cao et al., 2009; Moraveji et al., 2013).

Fig. 3 demonstrates the overall gas holdup in the system for different packing sizes with varying superficial gas velocity. It shows that the gas holdup monotonously increases with the increase of superficial gas velocity. Schafer et al (2002) believed that is because higher superficial gas velocity increases bubble collision frequency, which is beneficial for coalescence and the production of the larger bubbles.

It also can be seen from Fig. 3 that the gas holdup decreases with the increase of downcomer diameter in the whole. This tendency is consistent with Al-Masry and Abasaeed (1998), they explained that increasing the downcomer diameter is beneficial for liquid circulation, shortening the time the gas bubbles spend in the column, therefore, the gas holdup is decreased.

Besides the superficial gas velocity and downcomer diameter, packing size can also greatly alter the gas holdup. We can see that the gas holdup in the packed column is larger than that in an empty column. Compared to the two-phase system, when the packing size is 5 mm, the gas holdup has been increased by about 40 % at the high values of gas velocity, accordingly, 30 % for 14 mm packing and 20 % for 41 mm packing. It is partially due to a drop in the bubble velocity caused by the resistance of the packing, the flow tortuosity caused by packing leads longer path lengths for bubbles to travel. And it is partially due to the suppressed growth of bubbles in the presence of packing, a longer residence time is achieved for the small bubbles (Chen et al., 2017). The same tendency was observed by Nikakhtari and Hill (2005a, b, c).

In contrast to the conventional packed bubble column, it is found that the gas holdup increases with the decrease of packing size in the external-loop packed bubble column. That is because the liquid circulating velocity is smaller when the packing size is reduced, and the smaller pore path is easier to impede the rise of the bubbles, therefore, a higher gas holdup is obtained.

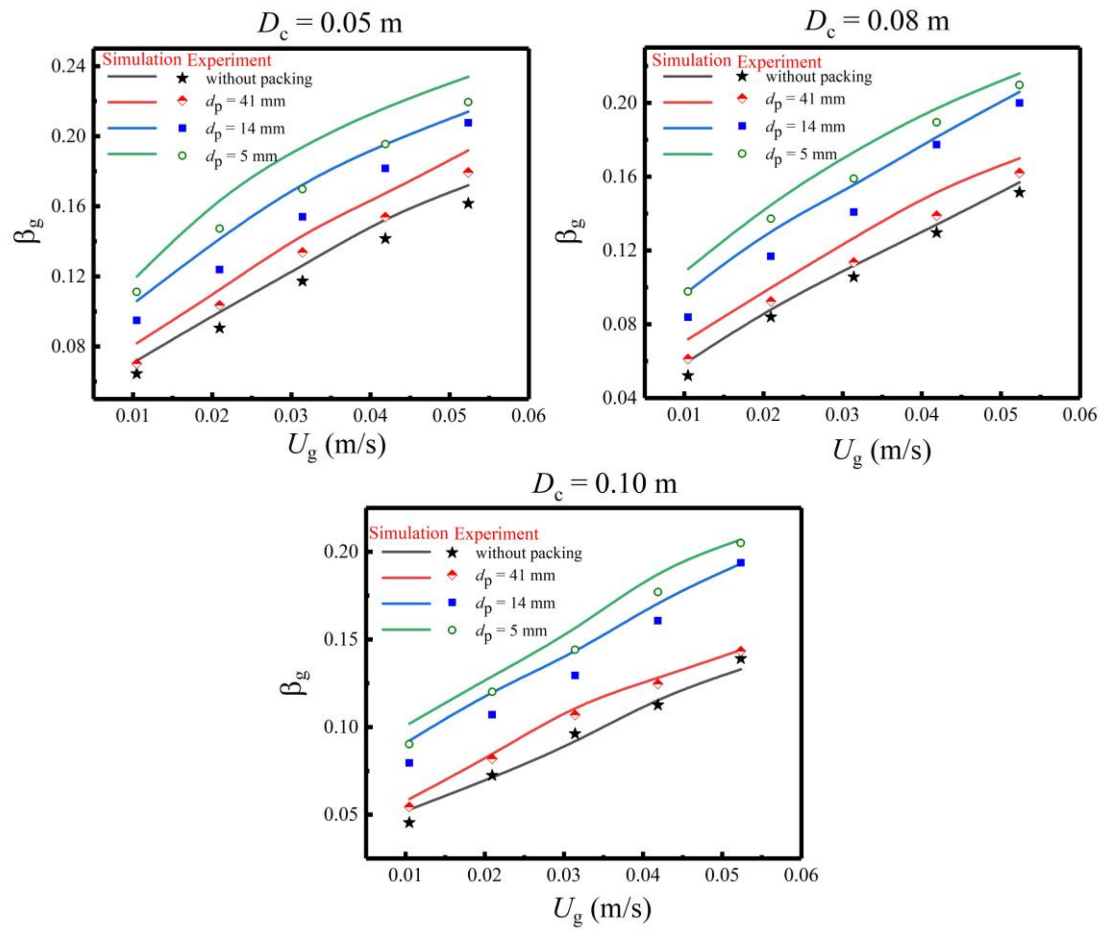

Fig. 3 The gas holdup under different conditions

It can be concluded that the overall gas holdup is affected by superficial gas velocity, packing characteristics and downcomer to riser diameter ratio, an empirical power-law correlation for estimating the overall gas hold-up is proposed.

$$\beta_g = \kappa \varepsilon^{n_1} \left(D_c/D_r\right)^{n_2} U_g^{\ n_3} \tag{14}$$

After the experimental data of the overall gas hold-up are fit by least-squares regression, the unknown parameters in eq. (14) are determined.

$$\beta_g = 0.54\varepsilon^{-0.84} \left(D_c/D_r\right)^{-0.21} U_g^{\ 0.55} \tag{15}$$

A comparison between predictions based on this correlation and the experimental data from this work is shown in Fig. 4 with a relative error of less than 25%.

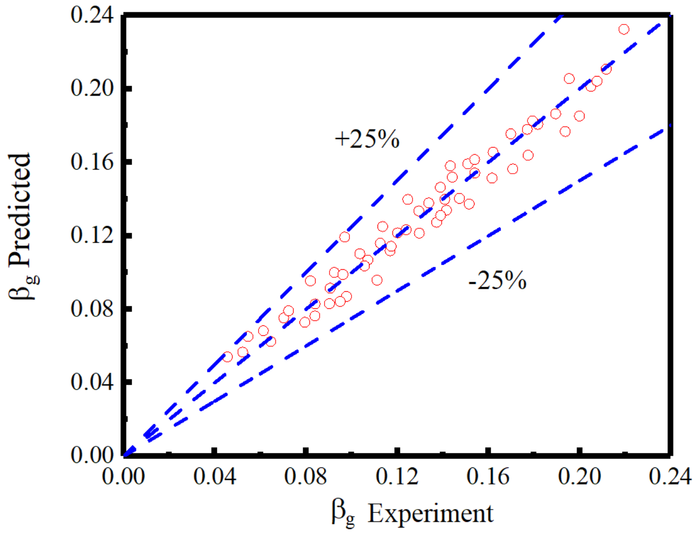

Fig. 4 Comparison of the experimental and predicted overall gas holdup

3.3 The liquid circulating velocity

Liquid circulating velocity in the dowmcomer, is considered as one of the most important parameters in structure design. The liquid circulating velocities in different operation conditions are illustrated in Fig. 5.

It is found that the liquid circulating velocity increases with the increase the superficial gas velocity, this is because that the liquid circulating velocity is governed by the ratio of driving force (the difference of gas holdup between the riser and downcomer) and resistance force (energy dissipation during the circulation) in the external-loop bubble column (Felice, 2005). When the superficial gas velocity increases, the gas holdup gets larger, which leads to an increased driving force, thus, the liquid circulating velocity increases.

With the addition of solid particles in the system, the gas holdup in the riser increases, the driving force becomes larger. However, the hindrance force of the liquid circulation is also increased by the increase of frictional loss due to the reduction of flow area. Thus, the effects of packing on the liquid circulating velocity are two-sided, both increase and decrease in the liquid circulating velocity can be found with the presence of packing compared to empty column. When superficial gas velocity is 0.052 m/s and downcomer diameter is 0.05 m. the liquid circulating velocity for empty column is 1.64 m/s, while it is 1.72 m/s for 41 mm packing, 1.16 m/s for 14 mm packing, and 0.54 m/s for 5 mm packing. A slight increase in liquid circulating velocity is found for 41 mm packing as the increase in gas holdup plays a major role, the same phenomenon is also observed by Moraveji et al (2013). However, in other cases, the increase of flow resistance is much greater than the increase of driving force, so the liquid circulating velocity in the packed column is less than that of empty column, which is a more common phenomenon in many researches (Meng et al., 2002; Nikakhtari and Hill, 2005a, b, c).

The flow resistance invariably increases with the decrease of packing size, which makes the liquid circulating velocity decrease with the decrease of packing size. It was observed a dramatic reduction in the liquid circulating velocity in the presence of 5 mm packing. For example, when the superficial gas velocity is 0.052 m/s, and the downcomer diameter is 0.10 m, the liquid circulating velocity for 41 mm packing is up to 1.18 m/s, while it is 0.81 m/s for 14 mm packing, however, it is only 0.15 m/s for 5 mm packing. This indicates that although the catalyst size can be reduced to increase the catalyst loading capacity and internal effectiveness factor, when the catalyst size is reduced to a certain extent, the liquid external circulation may not be realized due to the high resistance in the riser.

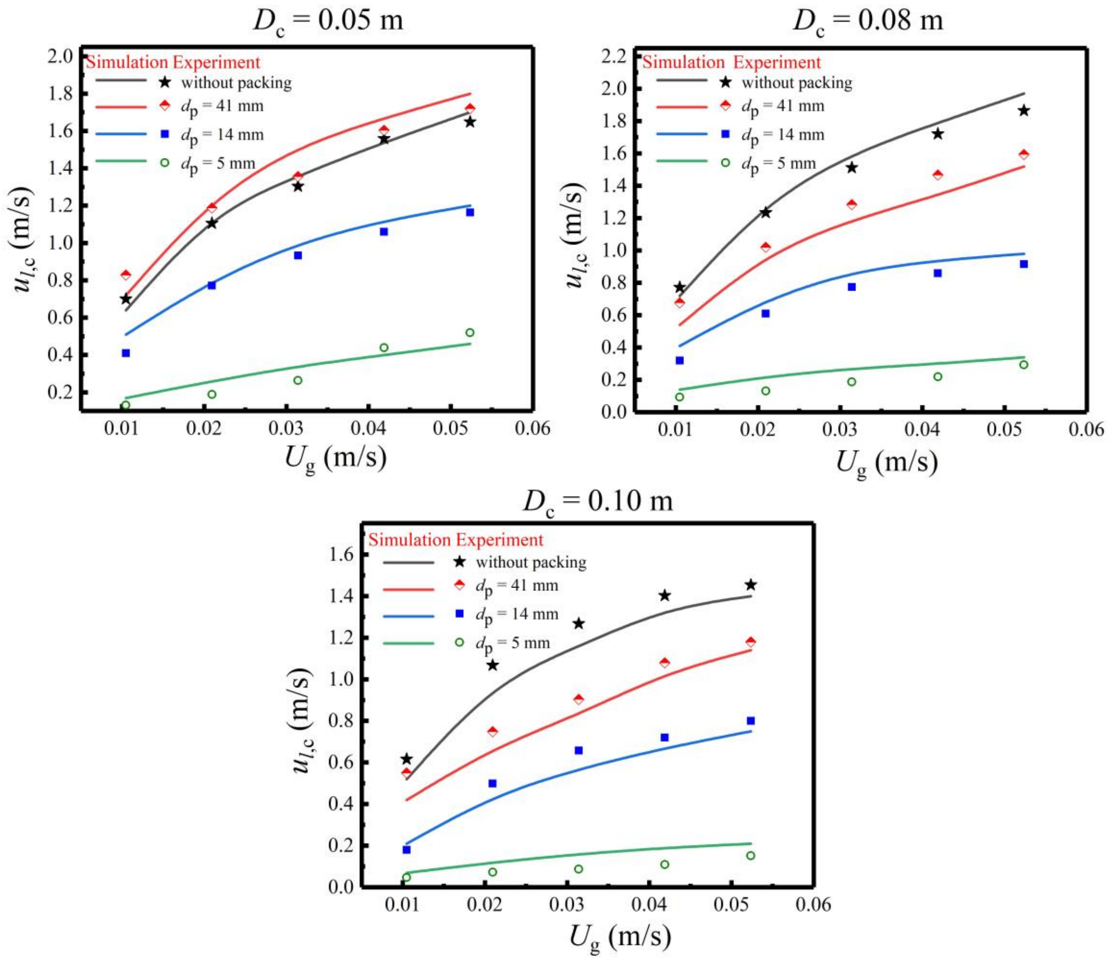

Fig. 5 The liquid circulating velocity in the downcomer under different conditions

It is better to discuss the effect of downcomer diameter on liquid circulation property combining with the liquid circulating volume flow rate (Seen in Fig. 6). It was found that except the packing size of 5 mm, the liquid circulating volume flow rate increases with downcomer diameter. That is because the resistance loss of liquid from the gas-liquid separator to the downcomer is smaller when the downcomer diameter gets larger (Al-Masry and Abasaeed, 1998).

However, when the packing size is 5 mm, the liquid circulating volume flow rate is the largest when the downcomer diameter is 0.08 m. The reason is that the liquid circulating velocity in the 0.10 m downcomer is too low due to the large cross section, which is not conducive to circulating in the high resistance of the fine packing.

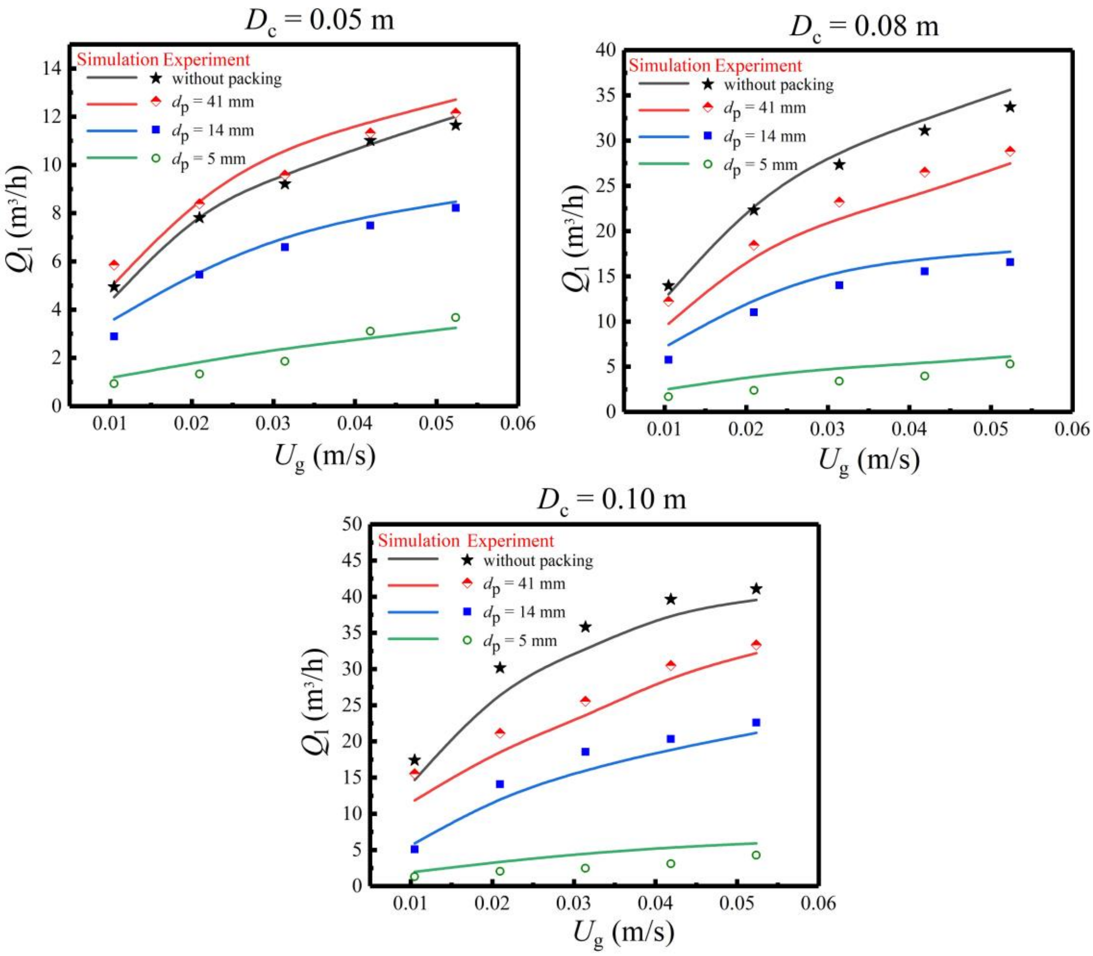

Fig. 6 The liquid circulating volume flow rate under different conditions

The liquid circulating velocities by simulations are in great agreement with those by experiments, and the simulations provide more information about liquid velocity distribution, which are shown in Fig. 7. The velocity streamlines verify that the liquid circulates between the riser and downcomer on the whole. In the empty column, there is a recirculation zone at the lower middle part of the riser, which is qualitatively consistent with Becker et al. (1994). Once the packing is added, the liquid velocity in the packing zone of the riser decreases due to the obstruction of the packing, and the packing also inhibits the liquid recirculation in the packing zone, however, a liquid recirculation zone occurs under the packing.

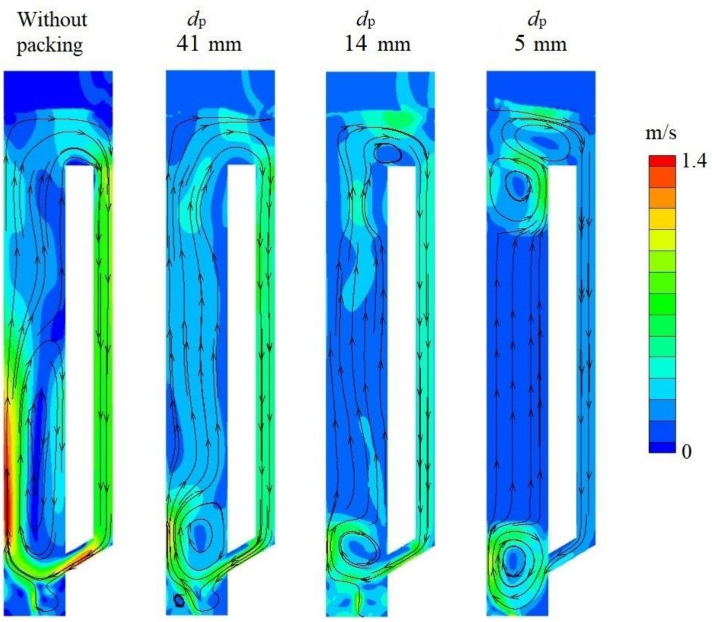

Fig. 7 The liquid velocity distribution by simulation in the external-loop reactor when D_c = 0.08 m and U_g = 0.01m/s

3.4 Volumetric mass transfer coefficient

The volumetric gas-liquid mass transfer coefficient (k_la) is also explored, and the results are shown in Fig. 8. It is clear that the volumetric gas-liquid mass transfer coefficient increases with the increase of superficial gas velocity. On the one hand, increasing superficial gas velocity increases the gas holdup, which provides more contact area for gas-liquid mass transfer. On the other hand, the increased gas holdup means greater driving force for the liquid external circulation, the turbulent kinetic energy of liquid increases, leading to the increase of k_l. All those factors contribute to increase the values of k_la.

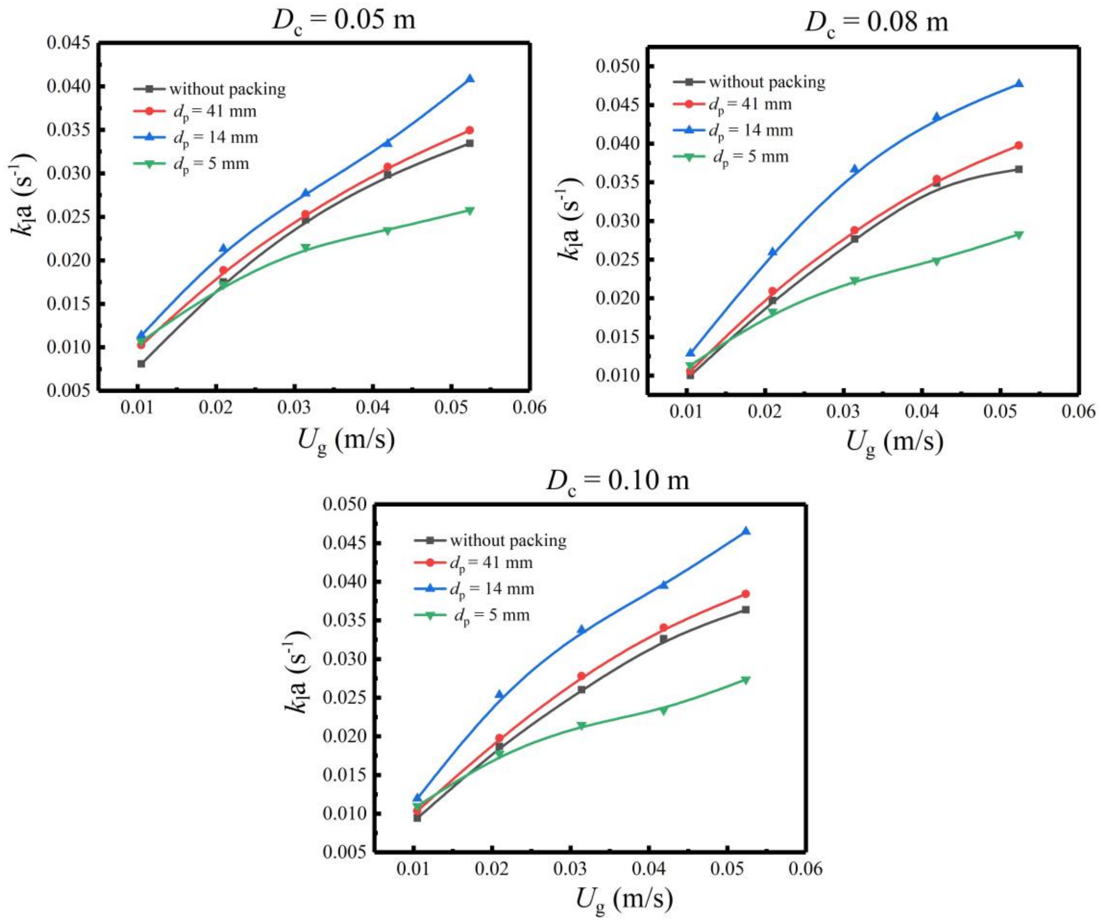

Fig. 8 The gas-liquid mass transfer coefficient under different conditions

The presence of packing on the k_la involves two competitive effects: 1) increase of gas holdup resulting from resistance of packing, which is favorable to increase of gas-liquid interfacial area, a; 2) decrease of liquid velocity and the turbulence intensity, which is unfavorable to any increase of gas-liquid mass transfer coefficient, k_l; Compared with the empty column, the k_la of packed column with 14 mm and 41 mm packing is larger due to the larger increase in gas holdup and less decrease in velocity. However, when the packing size is reduced to 5 mm, although the gas holdup is higher than the empty column, the liquid velocity decreases sharply. The decrease in k_l overleaps the increase in gas-liquid mass transfer area, so that the k_la of 5 mm packing is only half of that of 14 mm packing at high gas velocity, and even about 20-30% lower than that of empty column. For example, when the superficial gas velocity is 0.052 m/s and the downcomer diameter is 0.08 m, the k_la is 0.037 s^{-1} for empty column, while it is 0.040 s^{-1} for 41 mm packing, 0.048 s^{-1} for 14 mm packing, and 0.028 s^{-1} for 5 mm packing. The best packing size for gas-liquid mass transfer is 14 mm.

It can also be concluded that the k_la increased as follows in regard to downcomer diameter: 0.05 m < 0.10 m < 0.08 m. The downcomer of 0.08 m in diameter is most favorable for gas-liquid mass transfer, and this is a consequence of downcomer diameter on gas holdup and liquid circulating velocity.

4 Conclusions

In this study, an external-loop packed bubble column with Raschig ring packed in the riser is designed, which is used for a three-phase system with a strong exothermic reaction for the gas reactants, while the liquid only acts as an inert heat removal medium. The automatically external circulation of the inert liquid medium can greatly save energy of inserting liquid.

Variable factors affecting fluid dynamics are investigated. The overall gas holdup, liquid circulating velocity and gas-liquid mass transfer coefficient were respectively measured by volume expansion method, tracer-response method and dynamic oxygen-absorption technique. CFD simulation with the Euler-Euler two-fluid method was used to predict the liquid circulating velocity by treating the packing as a porous medium.

A comparative analysis of fluid dynamics in packed column and in a conventional empty column has been made. It is found that the gas holdup in the packed column is larger than that in the empty column, which provides more diving force for liquid external circulation. However, the resistance of liquid external circulation is also increased due to packing. Thus, the effect of packing on liquid circulating velocity are two-sided, liquid circulating velocity may increase or decrease.

In an external-loop packed bubble column, the gas holdup increases with the decrease of packing size, while the liquid circulating velocity decreases with the decrease of packing size. This tendency makes the maximum mass transfer coefficient to be obtained when the packing size is 14 mm. When the packing size is 5 mm, the maximum liquid circulating velocity and gas-liquid mass transfer coefficient are found when the downcomer diameter is 0.08 m. Finally, a power-law relationship for overall gas hold-up in the riser is employed in the paper, which give good agreement with experimental data.

Acknowledgment

The authors are grateful to the financial supports from and the National Key R&D

Program of China (No. 2019YFC1906705) and the National Natural Science Foundation of China (No. 21676085).

Nomenclatures

Latin symbols

C_l instantaneously dissolved oxygen concentration, g/m^3

C^* saturation dissolved oxygen concentration, g/m^3

C_0 initial dissolved oxygen concentration, g/m^3

d_p Effective diameter of Raschig ring, m

d_b diameter of bubble, m

D_c diameter of downcomer, m

D_r diameter of the riser, m

Q_l liquid circulating volume flow rate, m^3/h

t time, s

U_g superficial gas velocity, m/s

$u_{l,c}$ liquid circulating velocity in the downcomer, m/s

$\overrightarrow{u_k}$ velocity vector of phase k, m/s

β_k volume fraction of phase k, dimensionless

$k_l a$ volumetric gas-liquid mass transfer coefficient, s^{-1}

ρ_k density of phase k, kg/m^3

σ gas-liquid surface tension, N/m

$\overline{\overline{\tau}}_k$ average stress tensor, Pa

E_1, E_2 Ergun constants, dimensionless

$\overrightarrow{F_{g,s}}$, $\overrightarrow{F_{l,s}}$ gas-solid and liquid-solid interaction force, N/m^3

$\overrightarrow{F_{g,l}}$, $\overrightarrow{F_{l,g}}$ gas–liquid interaction force, N/m^3

$K_{k,s}$ momentum exchange coefficient of phase, kg/m^3/s

$K_{g,l}$ gas–liquid interaction coefficient, kg/m^3/s

p pressure, Pa

Eo Eötvös number, dimensionless

subscript

k=g, l gas and liquid

References

Al-Masry, W.A., Abasaeed, A.E., 1998. On the scale-up of external loop airlift reactors: Newtonian systems. Chemical Engineering Science 53, 4085-4094.

Atta, A., Roy, S., Nigam, K.D.P., 2007. Investigation of liquid maldistribution in trickle-bed reactors using porous media concept in CFD. Chemical Engineering Science 2007, 7033-7044.

Becker, S, Sokolichin, A., Eigenberger, G., 1994. Gas-liquid flow in bubble columns and loop reactors: Part II. Comparison of detailed experiments and flow simulations. Chemical Engineering Science 49, 5747-5762.

Bian, Q., Tang, X.J., Hu, L.F., Wang, S.B., Zhang, Z.Z., 2016. Hydrodynamic characteristics in an external loop airlift slurry reactor. China Petroleum Processing and Petrochemical Technology 18(3), 83-90.

Bordas, M.L., Cartellier, A., Sechet, P., Boyer, C., 2006. Bubbly flow through fixed beds: Microscale experiments in the dilute regime and modeling. AIChE Journal

52, 3722-3743.

Boyer, C., Volpi, C., Ferschneider, G., 2007. Hydrodynamics of trickle bed reactors at high pressure: two-phase flow model for pressure drop and liquid holdup, formulation and experimental validation. Chemical Engineering Science 62, 7026-7032.

Cao, C., Zhao, Y., Dong, S., Guo, Q., 2009. Dimensional similitude for scale-up of hydrodynamics in a gas-liquid-(solid) EL-ALR. Chemical Engineering Science 64(23), 4992-5001.

Chen, Z.X., Yang, J., Ling, D., Liu, P., Ilankoon, I. M. S. K., Huang, Z.B., Cheng, Z.M., 2017. Packing Size Effect on the Mean Bubble Diameter in a Fixed Bed under Gas-Liquid Concurrent Upflow. Industrial & Engineering Chemistry Research 56(45), 13490-13496.

Chisti, Y., Moo-Young, M., 1993. The airlift bioreactor with packed beds of immobilized biocatalysts: Theoretical evaluation of the liquid circulation performance. Transactions of the Institution of Chemical Engineers 71, 209-214.

Chisti, Y., Moo-Young, M., 1994. Anchorage dependent animal cell culture in packed beds with airlift driven liquid circulation: a theoretical analysis of oxygen transfer and comparison with stirred tank microcarrier culture system. Transactions of the Institution of Chemical Engineers 72C, 92-94.

Collins, J.H., Sederman, A.J., Gladden, L.F., Afeworki, M., Kushnerick, J.D., Thomann, H., 2017. Characterising gas behaviour during gas-liquid co-current up-flow in packed beds using magnetic resonance imaging. Chemical Engineering Science

157, 2-14.

Deshpande, S.S., Walker, J., Pressler, J., Hickman, D., 2018. Effect of packing size on packed bubble column hydrodynamics. Chemical Engineering Science 186, 199-208.

Dhaouadi, H., Poncin, S., Hornut, J.M., Wild, G., 2006. Solid effects on hydrodynamics and heat transfer in an external loop airlift reactor. Chemical Engineering Science 61, 1300 -1311.

Fakhari, M.E., Moraveji, M.K., Davarnejad, R., 2014. Hydrodynamics and Mass Transfer of Oily Micro-emulsions in an External Loop Airlift Reactor. Chinese Journal of Chemical Engineering 22(3), 267-273.

Felice, R.D., 2005. Liquid circulation rates in two- and three-phase external airlift reactors. Chemical Engineering Journal 109, 49-55.

Gavrilescu, M., Tudose, R.Z., 1997. Mixing studies in external-loop airlift reactors. Chemical Engineering Journal 66, 97-104.

Geng, S.J., Li, Z., Liu, H.Y., Yang, C., Gao, F., He, T.B., Huang, Q.S., 2020. Hydrodynamics and mass transfer in a slurry external airlift loop reactor integrating mixing and separation. Chemical Engineering Science 211, 115294.

Guo, Y.X., Rathor, M.N., Ti, H.C., 1997. Hydrodynamics and mass transfer studies in a novel external-loop airlift reactor. Chemical Engineering Journal 67, 205-214.

Hamood-ur-Rehman, M., Dahman, Y., Ein-Mozaffari, F., 2012a. Investigation of mixing characteristics in a packed-bed external loop airlift bioreactor using tomography images. Chemical Engineering Journal 213, 50-61.

Hamood-ur-Rehman, M., Ein-Mozaffari, F., Dahman, Y., 2012b. Dynamic and local gas holdup studies in external loop recirculating airlift reactor with two rolls of fiberglass packing using electrical resistance tomography. Journal of Chemical Technology and Biotechnology 88, 887-896.

Ishii, M., Zuber, N., 1979. Drag coefficient and relative velocity in bubbly, droplet or particulate flows. AIChE Journal 13(6), 1219-1221.

Jalilnejad, E., Vahabzadeh, F., 2014. Use of a packed-bed airlift treactor with net draft tube to study kinetics of naphthalene degradation by Ralstonia eutropha. Environmental Science and Pollution Research 21, 4592-4604.

Jo, D., Revankar, S.T., 2009. Bubble mechanisms and characteristics at pore scale in a packed-bed reactor. Chemical Engineering Science 64, 3179-3187.

Jo, D., Revankar, S.T., 2010. Effect of coalescence and breakup on bubble size distributions in a two-dimensional packed bed. Chemical Engineering Science 65, 4231-4238.

Lamine, A., Serrano, M., Wild, G., et al., 1995. Influence of viscosity and foaming properties on heat-transfer in packed-bed with cocurrent upflow of gas and liquid. Chemical Engineering Research and Design 73 (3), 280-285.

Lappalainen, K., Gorshkova, E., Manninen, M., Alopaeus, V., 2011. Characteristics of liquid and tracer dispersion in trickle-bed reactors: Effect on CFD modeling and experimental analyses. Computers and Chemical Engineering 35, 41-49.

Lappalainen, K., Manninen, M., Alopaeus, V., 2009. CFD modeling of radial spreading of flow in trickle-bed reactors due to mechanical and capillary dispersion.

Chemical Engineering Science 64, 207-218.

Lechowska, J., Kordas, M., Konopacki, M., Fijalkowski, K., Drozd, R., Rakoczy, R., 2019. Hydrodynamic studies in magnetically assisted external-loop airlift reactor. Chemical Engineering Journal 362, 298-309.

Ling, D., Liu, P., Cheng, Z.M., 2017. Methanol Synthesis in a Three-Phase Catalytic Bed Under Nonwetted Condition. AIChE Journal 63(1), 226-237.

Liu. M., Zhang, T.W., Wang, T.F., Yu, W., Wan, J.F., 2008. Experimental study and modeling on liquid dispersion in external-loop airlift slurry reactors. Chemical Engineering Journal 139, 523-531.

Meng, A.X., Hill, G.A., Dalai, A.K., 2002. Hydrodynamic Characteristics in an External Loop Airlift Bioreactor Containing a Spinning Sparger and a Packed Bed. Industrial & Engineering Chemistry Research 41, 2124-2128.

Milivojevic, M., Pavlou, S., Bugarski, B., 2012. Liquid velocity in a high-solids-loading three-phase external-loop airlift reactor. Journal of Chemical Technology and Biotechnology, 1529-1540.

Moreira, M.F., Freire, J.T., 2003. Influence of gas and liquid flow rates and the size and shape of particles on the regime flow maps obtained in concurrent gasliquid downflow and upflow through packed beds. Industry and Engineering Chemistry Research 42(4), 929-936.

Moraveji, M.K., Fakhari, M.E., Mohsenzadeh, E., Davarnejad, R., 2013. Hydrodynamics and oxygen mass transfer in a packed bed split-cylinder airlift reactor containing dilute Alcoholic solutions. Heat Mass Transfer 49, 11-19.

Moraveji, M.K., Gharib, J., 2014. Hydrodynamics and mass transfer study of oilwater micro-emulsion in a three phase external loop airlift reactor, RSC Advance 4, 62347-62355.

Nikakhtari, H., Hill, G.A., 2005a. Volatile Organic Chemical Mass Transfer in an External Loop Airlift Bioreactor with a Packed Bed. Industrial & Engineering Chemistry Research 44, 9299-9306.

Nikakhtari, H., Hill, G.A., 2005b. Hydrodynamic and oxygen mass transfer in an external loop airlift bioreactor with a packed bed, Biochemical Engineering Journal 27, 138-145.

Nikakhtari, H., Hill, G.A., 2005c. Enhanced Oxygen Mass Transfer in an External Loop Airlift Bioreactor Using a Packed Bed. Industrial & Engineering Chemistry Research 44, 1067-1072.

Papalas, T., Antzaras, A.N., Lemonidou, A.A., 2020. Intensified steam methane reforming coupled with Ca-Ni looping in a dual fluidized bed reactor system: A conceptual design. Chemical Engineering Journal 382, 122993.

Pronczuk, M., Bizon, K., 2019. Investigation of the liquid mixing characteristic of an external-loop hybrid fluidized-bed airlift reactor. Chemical Engineering Science 210, 115231.

Salmi, T., Carucci, J.H., Roche, M., Eranen, K., Warna, J., Murzin, D., 2013. Microreactors as tools in kinetic investigations: Ethylene oxide formation on silver catalyst. Chemical Engineering Science 87, 306-314.

Schafer, R., Marten, C., Eigenberger, E., 2002. Bubble size distributions in a bubble column reactor under industrial conditions. Experimental Thermal and Fluid science 26, 595-604.

Silapakul, S., Powtongsook, S., Pavasant, P., 2005. Nitrogen Compounds Removal in a Packed Bed External Loop Airlift Bioreactor. Korean Journal and Chemical Engineering 22(3), 393-398.

Sivakumar, V., Nirmala, G.S., Murugesan, T., 1999. Gas phase hold up in gas-liquid cocurrent upflow packed bubble columns at low Reynold's number. Bioprocess Engineering, 21, 41-43.

Solomenko, Z., Haroun, Y., Fourati, M., Larachi, F., Boyer, C., Augier, F., 2015. Liquid spreading in trickle-bed reactors: Experiments and numerical simulations using Eulerian-Eulerian two-fluid approach. Chemical Engineering Science 126, 698-710.